

SPIC base 2000  
San Jose  
22/1/00

1956

## Distortion correcting holographic resonators

*J. Hendricks, S. Mailis, D. P. Shepherd, A. C. Tropper, G. J. Crofts\*, M. Trew\*, M. J. Damzen\* and R. W. Eason*

Optoelectronics Research Centre,  
University of Southampton, Highfield,  
Southampton SO17 1BJ, U.K.  
Tele. No. : (+44) 01703 594527  
Fax. : (+44) 01703 593142  
Email : [jmh@orc.soton.ac.uk](mailto:jmh@orc.soton.ac.uk)

\*The Blackett Laboratory, Imperial College,  
London SW7 2BZ, U.K.

### ABSTRACT

High phase conjugate reflectivities ( $R > 10,000\%$ ) have been achieved through degenerate four-wave mixing in a cw diode-side-pumped Nd:YVO<sub>4</sub> amplifier and the interactions have been successfully modelled. This four-wave mixing geometry has subsequently been used in the design of a phase-conjugate resonator operating with a single-longitudinal mode TEM<sub>00</sub> near-diffraction limited output of  $> 7$  W, which is capable of correcting for severe intra-cavity phase distortions.

**Keywords:** Degenerate four-wave mixing, Phase-conjugation, Gain-grating, Distortion correction, Self-adaptive, Spatial hole-burning, Diode-pumped laser.

### 1. INTRODUCTION

Diode-pumped solid-state lasers are cheap and robust lasers that have found wide acceptance in many applications that would otherwise require larger more expensive alternatives. The output of the diode laser itself has poor spatial qualities and hence poor focusability, which severely limits its uses, but can be used to pump a second laser. This laser, often consisting of a solid-state crystal gain medium can have a more controlled spatial output and thus a dramatically improved beam quality and brightness. Problems occur however when we want to increase the output power to arbitrarily high values; as the crystal is pumped harder distortions (thermal lensing, stress birefringence etc.) are introduced to the modes propagating inside the cavity<sup>1</sup>, and the spatial quality of the output beam deteriorates. Phase conjugation has been used extensively in the past to correct for distortions present in high-average power laser cavities. The distortion correcting properties of phase conjugate waves allow for intracavity distortions such as thermal lensing in solid-state media to be corrected for and produce high spatial quality laser outputs. Four-wave mixing (FWM) in gain media is one technique that can be used to produce phase conjugate waves and has been successfully demonstrated in flash-lamp-pumped Nd:YAG amplifiers<sup>2</sup>, quasi-cw diode-pumped Nd:YAG and Nd:YVO<sub>4</sub> amplifiers<sup>3,4</sup> and laser-pumped titanium-doped sapphire<sup>5</sup>. In this report we detail a resonator operating with an output of  $>7$  W that is capable of correcting for intra-cavity distortions using phase-conjugation by saturable-gain four-wave mixing.

## 2. THEORY

### 2.1. Phase Conjugate waves

The key to correcting aberrations inside the resonator is the use of optical phase conjugation. Figure 1. shows a signal wave with a convex spherical wavefront that is incident on a conventional plane mirror. The reflected wave is still convex spherical and continues to diverge. The mirror has only reversed the sign of the component of the wave  $k$ -vector that is perpendicular to the plane of the mirror.

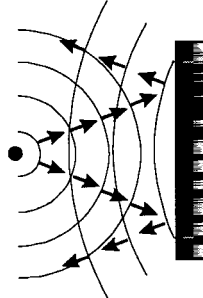


Figure 1. A diverging wave incident on a conventional mirror continues to diverge after reflection from the mirror.

If the same initial wavefront is incident on a phase-conjugate mirror (PCM), however, as shown in figure 2., the PCM has the property of being able to reverse all three cartesian components of the  $k$ -vector of the incident wavefront, and so all the reflected components are reflected back towards the point from which they originally emanated. In the case of the incident convex spherical wavefront (travelling from left to right) the reflected beam is a concave spherical wavefront travelling from right to left, at all points remaining the exact replica of the incident wave at that point but travelling in the opposite direction i.e. the phase of the wave has been reversed.

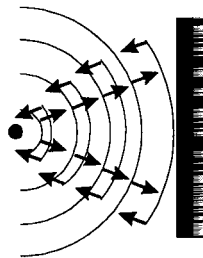


Figure 2. A phase-conjugate mirror reflects the phase-conjugate of an incident wave. An incident diverging wave will reflect as a converging wave which then travels back towards the point from which the original beam came from.

### 2.2. Distortion correction theorem

An ideal phase conjugate mirror should be able to reflect the phase conjugate of any arbitrary wave incident on it. Figure 3. shows an initial plane wave, travelling from left to right, which has been distorted by a phase distorting medium. This distorted wave is then incident on a phase-conjugate mirror. The reflected phase-conjugate wave then travels back towards the distorting medium. Now the distorted phase-conjugate wave passes back through the same medium, at all points exactly retracing those distortions imposed on the forward going wave.

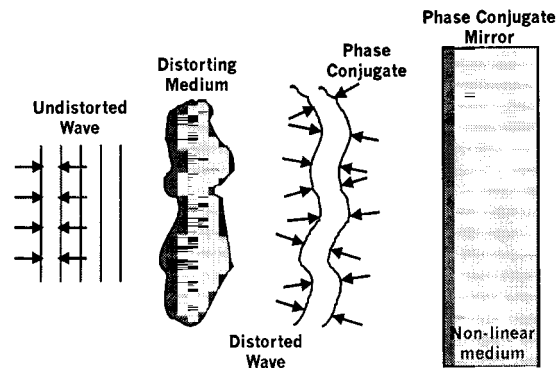


Figure 3. Schematic showing the distortion correcting properties of phase-conjugate waves. When the phase-conjugate wave is double-passed back through the distorting medium any phase aberrations are removed, thereby regenerating the original undistorted wave.

On re-traversing the distorter the backward going wave is now ‘healed’ of any distortions and we have a plane wave again. This argument can clearly be generalised to any initial incident wave<sup>6</sup>, and to the situation where the distorter and PCM are within the same medium.

### 2.3. Production of PC waves Via a Bragg grating

So far we have discussed some of the properties of phase-conjugate waves without actually discussing the mechanisms by which they are produced. Phase-conjugation has been studied extensively in stimulated Raman<sup>7,8</sup> and stimulated Brillouin<sup>9</sup> scattering interactions. The technique we use is the non-linear process of saturable-gain degenerate four-wave mixing (DFWM) in a solid-state amplifier. Here, three waves are all incident together within a non-linear mixing region where they couple to form a fourth output wave which is the phase-conjugate of one of the three incident waves. Figure 4. shows the standard geometry employed.

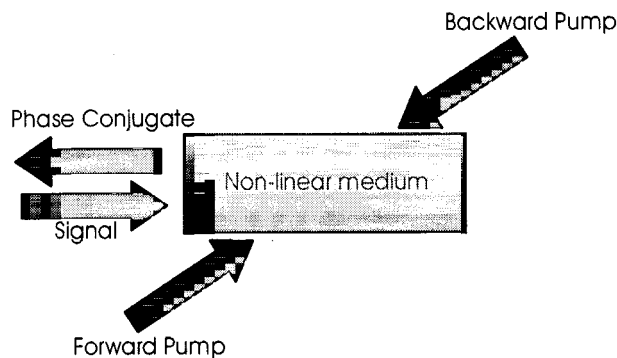


Figure 4. The standard four-wave mixing geometry. Three incident waves, the forward pump, backward pump and signal couple within the non-linear medium to produce a fourth wave which is the phase-conjugate of the signal wave.

It is convenient to look at the mixing process from a holographic viewpoint. The forward pump (FP) and the signal (S) are directed towards the non-linear medium where they interfere with each other and modulate a property of the medium according to the intensity pattern of the interfering waves. We now have a volume transmission diffraction grating inside the medium in which is encoded all the phase information of the FP and S waves. This grating is now simultaneously read out by another wave, the backward pump (BP), which is the phase-conjugate of the FP. This restriction also ensures that the BP is

exactly Bragg matched to 'read out' the grating. The diffracted wave (PC) is then the phase-conjugate of the incident signal (S) wave.

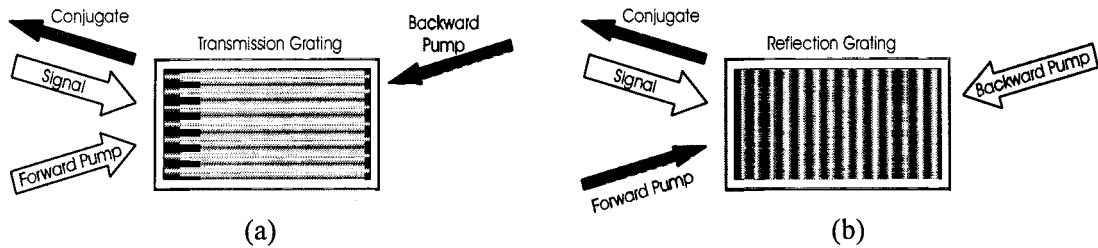


Figure 5. Schematic showing the two grating geometries. (a) The first, a transmission grating, is formed by the interference of the signal and forward pump. This is then read out by the backward pump to produce the conjugate. (b) The second, a reflection grating, is formed by interference between the signal and backward pump. This is read out by the forward pump.

Viewed as a 'black box' geometry we have a phase-conjugate mirror consisting of the non-linear (grating-supporting) medium and the FP and BP, from which a signal is reflected to produce its phase-conjugate wave. The reflectivity of the PCM is defined as the ratio of phase-conjugate power to signal power. The four-wave mixing process allows reflectivities  $> 1^{10}$  and in the case of four-wave mixing in a gain medium reflectivities of very much greater than unity can be achieved<sup>11</sup>. The case described above is that of a transmission grating, figure 5 (a) formed between the FP and S and read by the BP. A reflection grating between the BP and S which is read out by the FP can also occur at the same time as the transmission grating, figure 5 (b).

#### 2.4. Formation of the grating (spatial hole burning)

The property of the non-linear medium above that allows us to form a grating is that of gain saturation in an inverted medium. The non-linear crystal is pumped to produce an inverted population.

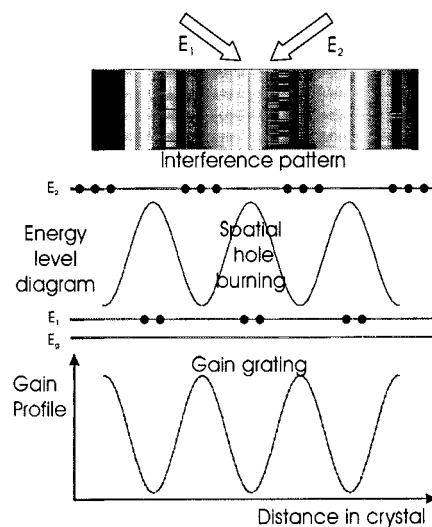


Figure 6. Formation of a gain-grating. The interference of two waves  $E_1$  and  $E_2$  modulates the gain of the inverted medium via spatial hole burning.

The interference pattern between the FP and S inside the inverted medium causes the gain to be modulated, via spatial hole burning, lowering the gain in places where there is an interference maximum and having little or no effect where there is an interference minimum, figure 6.

### 3. EXPERIMENTAL

#### 3.1. Four-wave mixing experiments

Figure 7. shows the experimental setup used to determine the phase-conjugate reflectivities that could be achieved in a gain four-wave mixing geometry. The gain medium used for the experiment was a 1.1 at % Nd doped YVO<sub>4</sub> a-cut crystal with dimensions of 3 x 5 x 20 mm. This was antireflection coated on both b sides for the pumping wavelength and antireflection coated on both a sides for the lasing wavelength (1064 nm). The crystal was side-pumped with a 20 W CW laser-diode which was fibre lensed and able to deliver an 18 W collimated beam at 808 nm. The output polarisation of the diode was then rotated with a  $\lambda/2$  wave plate to be parallel with the c-axis of the crystal giving a maximum pump absorption ( $\alpha = 30 \text{ cm}^{-1}$ ). This output was then focused onto one of the b-sides of the crystal using a 12.3 mm cylindrical lens. The FP, BP and S were all obtained from a single-longitudinal mode Nd:YVO<sub>4</sub> laser that produced a diffraction limited beam of 300 mW output power at 1064 nm. Reflecting the beam off the pumped b-side ensured a near uniform gain across the beam profile and allowed us to access the regions of higher gain (those nearer the pumped face)<sup>12, 13</sup>. The signal, forward pump and backward pump were all focussed into the crystal to a calculated spotsize of 38  $\mu\text{m}$ , and arranged so that they all overlapped at the focal point of the lens.

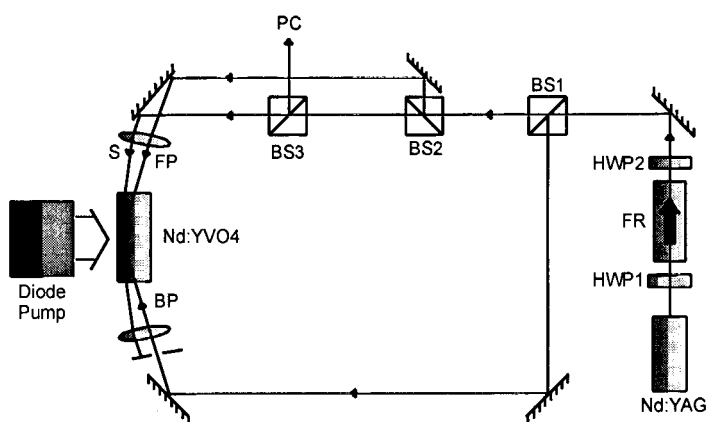


Figure 7. Schematic diagram of the four-wave mixing scheme used to measure phase-conjugate reflectivities in Nd:YVO<sub>4</sub>.

The backward pump was made to counter propagate with respect to the forward pump ensuring it was Bragg matched to the transmission grating formed between the signal and forward pump, and that the forward pump was Bragg matched to the reflection grating formed between the signal and the backward pump. A beamsplitter (BS3) was then used to pick off the phase conjugate of the signal beam and phase-conjugate reflectivities for different small signal single pass gains were plotted. All interacting beams were polarised parallel to the crystal c-axis to access the highest emission cross-section. Figure 8. shows the crystal orientation and the polarisation of the beams.

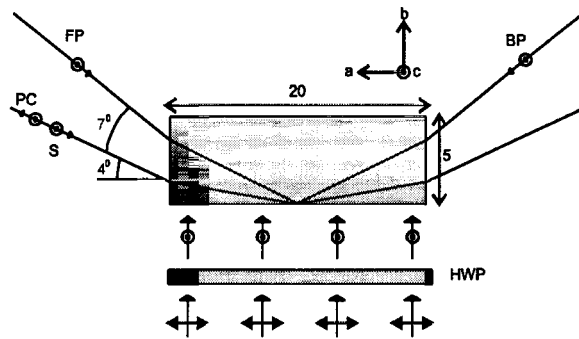


Figure 8. Diagram showing the beam geometry and polarisations relative to the crystal axis.

### 3.2. Four-wave mixing results

Figure 9. shows the experimental results of the phase-conjugate reflectivity as a function of the forward pump intensity normalised to the saturation intensity,  $I_{sat}$ , of Nd:YVO<sub>4</sub> ( $I_{sat}$  for Nd:YVO<sub>4</sub> is  $\sim 903 \text{ W cm}^{-2}$ ). This was done for three pumping levels of the amplifier by altering the current to the pump diode. Also shown on the graph are the theoretical results of a four-wave mixing model (lines) which show good agreement with the experimental results and is detailed in reference<sup>11</sup>. A maximum reflectivity of 8.2 was observed for a small-signal single-pass gain ( $G_{sig}$ ) of 1000<sup>11</sup>.

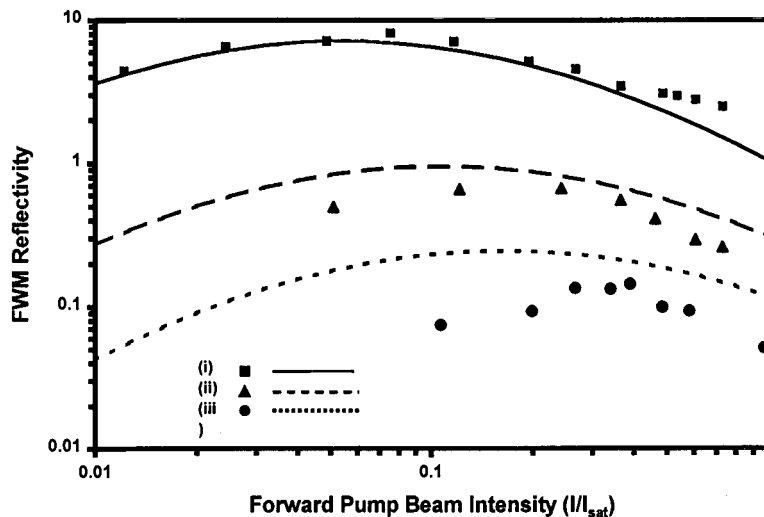


Figure 9. Phase-conjugate reflectivity versus intensity normalised to  $I_{sat}$  ( $\sim 903 \text{ W cm}^{-2}$ ) for small-signal gain values of (i)  $G_{sig} = 1000$ ,  $G_{pump} = 100$ ; (ii)  $G_{sig} = 150$ ,  $G_{pump} = 40$ ; (iii)  $G_{sig} = 45$ ,  $G_{pump} = 20$ . The points represent experimental values, and the curves represent the numerical modelling results.

More recent results, as shown in figure 10. yield reflectivities of  $\sim 100$ . This result was obtained by better overlap between the interacting beams and the pumped volume allowing greater four-wave mixing efficiency and greater extraction of available power.

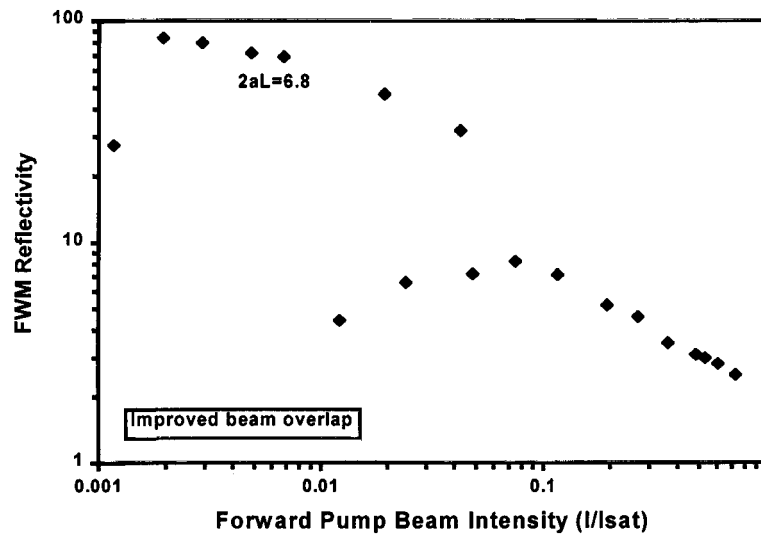


Figure 10. Phase-conjugate reflectivity versus intensity normalised to  $I_{\text{sat}}$  ( $\sim 903 \text{ W cm}^{-2}$ ). The latest results show FWM reflectivities greater than 10 times the previous reported maximum (also shown on the plot). These results were obtained from a better writing beam overlap inside the Nd:YVO<sub>4</sub> crystal.

### 3.3. Phase conjugating resonator

Figure 11. shows the geometry used to produce an adaptive laser resonator. In this setup a 1.1 at% Nd doped YVO<sub>4</sub> a-cut crystal with dimensions of 1 x 3 x 20 mm was pumped with a 25 W diode-laser. The diode was fibre-lensed and produced a collimated output of 23 W at 808 nm. The crystal a-sides were angled at  $\sim 2$  degrees to avoid parasitic lasing etc. The pumped b-side was antireflection coated for the pumping wavelength and the two a-sides were antireflection coated for the lasing wavelength (1064 nm) all other sides were inspection polished. The same 300 mW Nd:YVO<sub>4</sub> laser used before to produce the signal, forward and backward pump was used as a seeding source in this experiment.

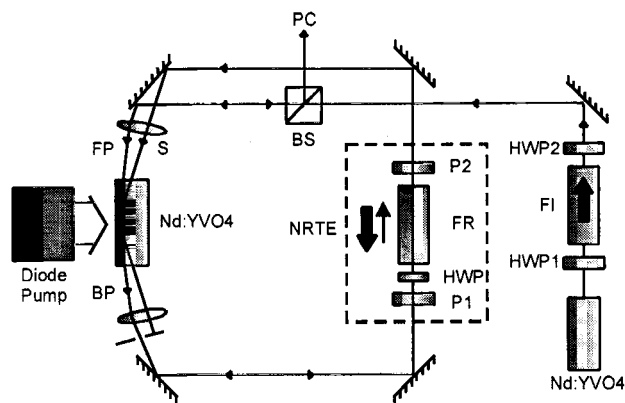


Figure 11. Schematic diagram of the seeded phase-conjugate resonator.

The gain grating is now formed by the self-intersection of the seed laser after a complete round-trip of the resonator. The output of the seed laser is directed towards the amplifier and becomes the forward pump.

This is then sent around the resonator loop where it picks up any phase distortions present in the loop and becomes the signal beam which is refocused into the gain region to overlap with the forward pump. The phase information of any distortions present in the loop are then encoded in the volume gain grating formed between the forward pump and signal. Amplified spontaneous emission (ASE) in the amplifier is now scattered off this grating to form the phase conjugate of the signal which retraces the path of the signal in a clockwise direction to become the backward pump which can again read out the grating to produce the phase conjugate of the signal beam. The resonator is 'closed' by the formation of the gain grating and begins to oscillate in the clockwise direction. The undiffracted part of the backward pump then becomes the resonator output. This geometry ensures that the backward pump is always perfectly Bragg matched to the gratings formed.

A non-reciprocal transmission element (NRTE) consisting of a  $\lambda/2$  wave plate (HWP) inside a faraday isolator (FR, P1 and P2) is placed in the loop so that the relative intensities of the forward pump and signal beams can be optimised to produce the largest modulation interference pattern and hence produce a gain grating with a large diffraction efficiency (the largest modulation occurs for waves of equal intensity at the point of interference). Although the NRTE induces a large loss in the anti-clockwise direction it still has near-unity transmission in the clockwise direction and allows the resonator to oscillate in that direction only.

### 3.4. Input-output characteristics

The seeded phase-conjugate resonator can be viewed as a phase-conjugating mirror with the incident beam being the seeded input and the phase-conjugate reflected beam being the resonator output. Figure 12. shows the phase-conjugate output of the resonator for varying seed input powers for a resonator whose maximum output is 3.2 W.

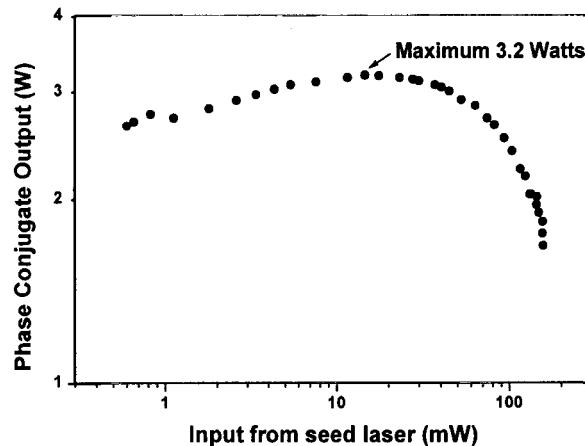


Figure 12. Graph showing the input-output characteristics of a seeded phase-conjugate resonator operating with a maximum output of 3.2 W. The diffraction efficiency of the gain-grating formed inside the Nd:YVO<sub>4</sub> falls considerably either side of this maximum due to under-saturation of the gain for values of input seed < ~15 mW and over-saturation for input seed values > ~15 mW.

For input values of the seed laser below the optimum value (~15 mW) the modulation depth of the interference pattern of the grating writing beams is small and hence the gain-grating also has a small modulation and therefore a small diffraction efficiency. For input values of the seed laser greater than the optimum value a high modulation depth of the interference pattern is produced but almost all of the available gain in the inverted Nd:YVO<sub>4</sub> is depleted leading to a small diffraction efficiency<sup>14</sup>.



### 3.5. Distortion correction

The resonator now consists of a phase-conjugate wave that is passing backwards through any distortions that distorted the original signal beam. From the distortion correction theorem, the phase-conjugate should become undistorted as it passes back through the system. This was tested by placing severe phase-distorting media within the resonator loop and observing the resonator output, figure 13.

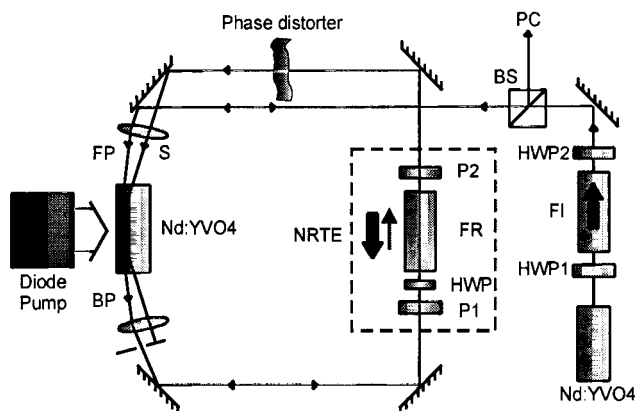


Figure 13. A phase-distortion was placed in the seeded resonator loop. The phase-distortions produced in the signal beam as it passes anti-clockwise around the loop are then encoded in the volume gain-grating. The phase-conjugate beam then passes clockwise through the distorter where the aberrations are removed in accordance with the distortion correction theorem.

The output of the resonator had a measured power in excess of 7.2 W with a  $M_x^2$  of 1.1 and  $M_y^2$  of 1.3; it was also found to operate in a single longitudinal mode. Figure 14. shows the undistorted resonator output (a), the effect of passing the beam through the distortion outside the resonator (b), and the observed resonator output with the distortion inside the resonator (c) respectively.

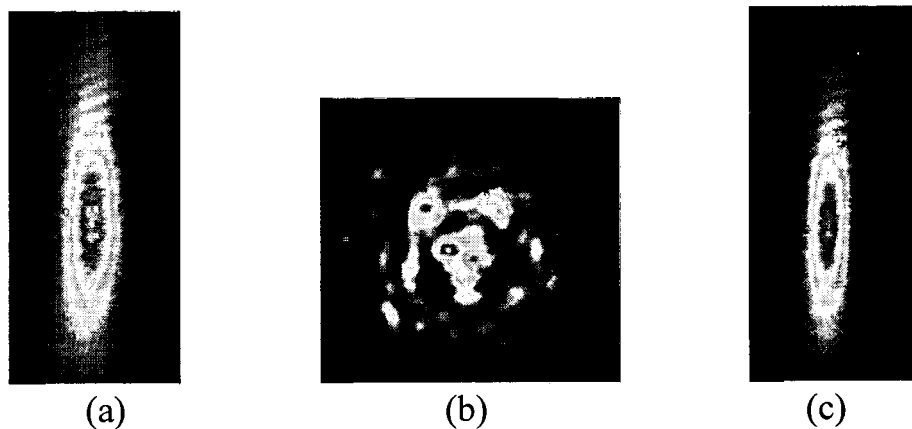


Figure 14. (a) The output of the seeded phase conjugate resonator. (b) The result of passing the input beam through the phase aberration external to the resonator cavity. (c) The Output of the resonator with the distortion inside the cavity.

### 3.6. Self-starting resonator operation

The seeded resonator geometry above can be adapted to produce a self-starting resonator by removing the seed laser and using an output-coupler (OC) in its place, figure 15.

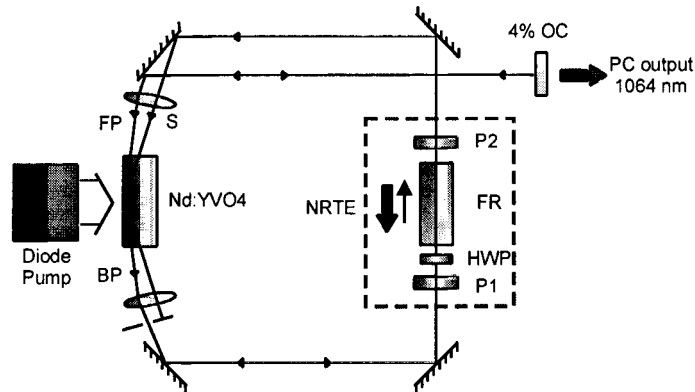


Figure 15. A self-starting resonator can be formed by replacing the seed laser and isolator with a 4% output coupler. The gratings are now formed by amplified spontaneous emission scattered of the output coupler to form the interacting beams.

Here all the interacting beams are produced by amplified spontaneous emission (ASE) from the pumped crystal that travels towards the 4% output-coupler and is then reflected back towards the crystal to produce the FP and the other beams. As with the seeded operation there is an optimum value of input (reflected light from the output-coupler) that gives the greatest output, and this conveniently lies around the value given by the Fresnel reflectivity of silica glass.

## 4. FUTURE WORK

Future work will include the incorporation of additional power amplifiers within the loop to increase the overall phase-conjugate output power from the resonator.

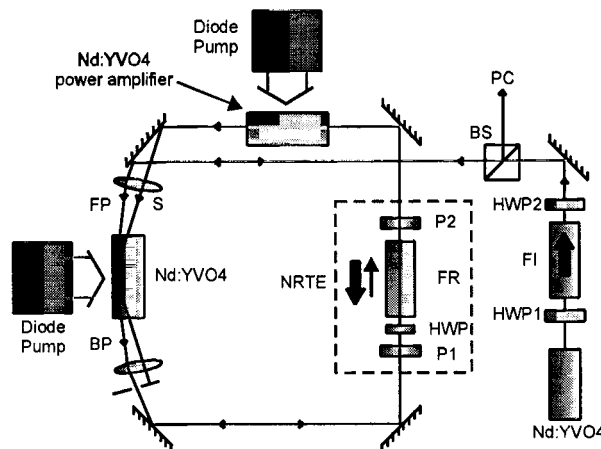


Figure 16. Additional power amplifiers can be incorporated in both the seeded and self-starting versions of the phase-conjugate resonator. Any aberrations introduced to the resonator mode by the new amplifier (thermal lensing, stress birefringence etc.) can be corrected for through the distortion correcting capabilities of the phase-conjugate resonator.

These power-amplifiers will introduce their own distortions to the modes of the resonator but both the seeded and self-starting phase-conjugate resonators have been shown to correct for phase aberrations placed within the resonator loop. Figure 16 shows the geometry of a seeded resonator with the additional amplifier elements present. Figure 17 shows the modelling of the output power of such a resonator as a function of the total power stored within the four-wave mixing crystal and the separate power amplifier. It can be seen that the power of the phase-conjugate output is proportional to the amount of available power in the resonator loop. So by placing the power amplifiers into the phase-conjugate resonator loop we should be able to achieve high power outputs with high quality beams.

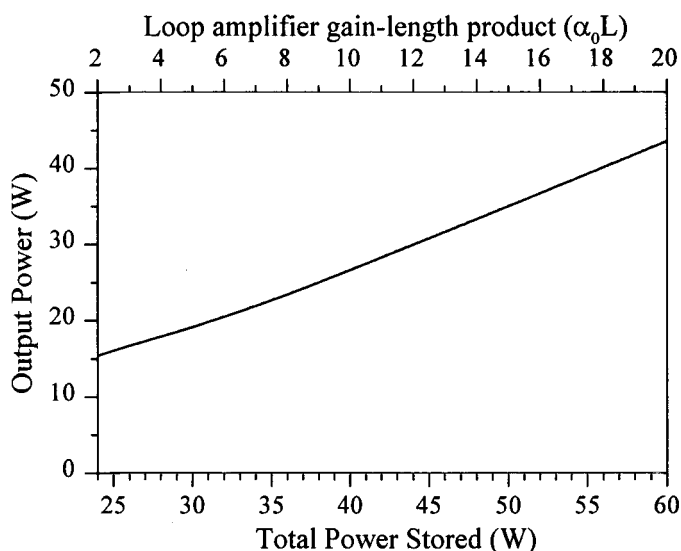


Figure 17. Graph of theoretical modelling results showing the output power available as a function of total stores power in the loop from a Phase conjugate resonator with an additional power amplifier.

Work is also underway looking at the possibility of an all-fibre geometry for the phase-conjugate resonator. Figure 18. shows a possible configuration of such a setup.

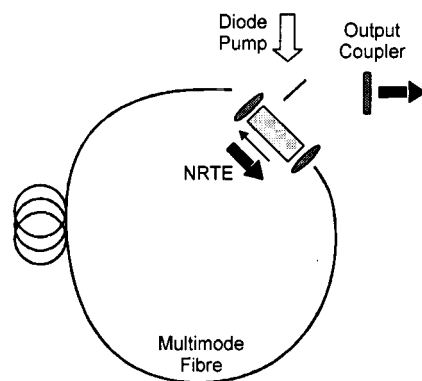


Figure 18. An all-fibre geometry phase-conjugate resonator.

The fibre geometry would use a large-core highly-multimode fibre which would give a large pumped volume, good power handling properties and relatively easy diode-coupling. This, of course, would normally lead to a highly multimode laser output but the phase-conjugate nature of such a system would give an output which was the phase-conjugate of the input to the fibre independent of what happens inside the fibre loop.

## 5. SUMMARY

In conclusion, phase conjugate reflectivities greater than 100 were obtained by degenerate four-wave mixing inside a gain-saturated Nd:YVO<sub>4</sub> diode-pumped amplifier. The FWM interactions have been modelled and have shown to be in good agreement with experimental observations. The high phase conjugate reflectivities obtained then lead to the realisation of a distortion correcting laser resonator operating with an output ~7 W TEM<sub>00</sub> single-longitudinal mode with  $M_x^2 < 1.3$  and  $M_y^2 < 1.1$ . This adaptive resonator was then shown to correct for large intra-cavity phase distortions both in a seeded and self-starting mode of operation. Finally work is underway on the incorporation of additional intra-cavity gain elements providing greater power output from the adaptive resonator. Possibilities of an all fibre geometry are also being investigated.

## ACKNOWLEDGMENTS

We thank the Engineering and Physical Sciences Research Council (EPSRC) for research funding under grants GR/L97209 and GR/L96455.

## REFERENCES

1. R. Weber, B. Neuenschwander, H. P. Weber, 'Thermal effects in solid-state laser materials', *Opt. Materials*, **11**, 245 (1999).
2. M. J. Damzen, R.P.M. Green and K.S. Syed, 'Self-adaptive solid-state laser oscillator formed by dynamic gain-grating holograms', *Opt. Lett.*, **20**, 1704 (1995).
3. A. Brignon, G. Feugnet, J.-P. Huignard and J.-P. Pochelle, 'Efficient degenerate four-wave mixing in a diode-pumped microchip Nd:YVO<sub>4</sub> amplifier', *Opt. Lett.*, **20**, 548 (1995).
4. P. Sillard, A. Brignon, J.-P. Huignard, J.-P. Pochelle, 'Self-pumped phase-conjugate diode-pumped Nd:YAG loop resonator', *Opt. Lett.*, **14**, 1093 (1998).
5. A. Minassian, G.J. Crofts and M.J. Damzen, *Opt. Lett.*, 'Self-starting Ti:sapphire holographic laser oscillator', **22**, 697 (1997).
6. A. Yariv, 'Optical electronics in modern communications', (Oxford university press, 1997).
7. A. I. Sokolovskaya, G. L. Brekhovskikh, A. D. Kudryavtseva, 'Light beams wavefront reconstruction and real volume image reconstruction of the object at the Stimulated Raman scattering', *Opt. Commun.*, **24**, 74 (1978).
8. R. W. Hellwarth, 'Theory of Stimulated Raman scattering', *Phys. Rev.*, **130**, 1850 (1963).
9. B. Y. Zel'dovich, V. I. Popovichev, V. V. Ragul'skii, F. S. Faizullov, 'Connection between the wave fronts of the reflected and excited light in stimulated Mandel'shtam-Brillouin scattering', *Sov. Phys. JETP Lett.*, **15**, 109 (1972).
10. A. Yariv, D. M. Pepper, 'Amplified reflection, phase conjugation, and oscillation in degenerate four-wave mixing', *Opt. Lett.*, **1**, 16 (1977).
11. S. Mailis, J. Hendricks, D. P. Shepherd, A. C. Tropper, N. Moore, R. W. Eason, G. J. Crofts, M. Trew, M. J. Damzen, 'High-phase-conjugate reflectivity (>800%) obtained by degenerate four-wave mixing in a continuous-wave diode-side-pumped Nd:YVO<sub>4</sub> amplifier', *Opt. Lett.*, **24**, 972 (1999).
12. J. E. Bernard, A. J. Alcock, 'High-efficiency diode-pumped Nd:YVO<sub>4</sub> slab laser', *Opt. Lett.*, **18**, 968 (1993).
13. J. E. Bernard, E. McCullough, A. J. Alcock, 'High-gain diode-pumped Nd:YVO<sub>4</sub> slab amplifier', *Opt. Commun.*, **109**, 109 (1994).
14. A. Brignon, J.-P. Huignard, 'Energy efficiency of phase conjugation by saturable-gain degenerate four-wave mixing in Nd:YAG amplifiers', *Opt. Commun.*, **119**, 171 (1995).